Key role of elastic vortices in the initiation of intersonic shear cracks

Sergey G. Psakhie,[1,2,3,4,*] Evgeny V. Shilko,[1,3] Mikhail V. Popov,[3,5] and Valentin L. Popov[3,4,5]
[1]*Institute of Strength Physics and Materials Science, Russian Academy of Sciences, Tomsk, Russia*
[2]*Skolkovo Institute of Science and Technology, 143025 Moscow, Russia*
[3]*Tomsk State University, 634050 Tomsk, Russia*
[4]*Tomsk Polytechnic University, Tomsk, 634050 Tomsk, Russia*
[5]*Berlin University of Technology, 10623 Berlin, Germany*
(Received 23 August 2014; revised manuscript received 10 December 2014; published 4 June 2015)

Using the particle-based method of movable cellular automata, we analyze the initiation and propagation of intersonic mode II cracks along a weak interface. We show that the stress concentration in front of the crack tip, which is believed to be the mechanism of acceleration of the crack beyond the speed of shear waves, is due to the formation of an elastic vortex. The vortex develops in front of the crack during the short initial period of crack propagation. It expands and moves away from the crack tip and finally detaches from it. Maximum stress concentration in the vortex is achieved at the moment of detachment of the vortex. The crack can accelerate towards the longitudinal wave speed if the magnitude of shear stresses in the elastic vortex reaches the material shear strength before vortex detachment. We have found that for given material parameters, the condition for the unstable accelerated crack propagation depends only on the ratio of the initial crack length to its width (e.g., due to surface roughness).

DOI: 10.1103/PhysRevE.91.063302 PACS number(s): 05.10.−a, 62.20.mm, 62.20.mt, 62.25.Mn

Dynamic propagation of mode II cracks (in-plane shear cracks) at speeds larger than the shear wave speed but smaller than the longitudinal wave speed (intersonic crack propagation) has been studied experimentally, theoretically, and numerically in the contexts of earthquakes, fracture of materials, and friction. The reason for intersonic crack propagation was found to be the stress concentration ahead of the crack tip [1–3]. The existence of a shear stress peak ahead of a mode II crack growing in the unstable regime was predicted analytically by Burridge [1]. In the following decades the development of such stress peaks was subject to detailed numerical modeling and laboratory experiments [2,4–8]. It was found that the stress peak arises during the initial phase of unstable crack growth and propagates ahead of the rupture front at the shear wave velocity [2]. Moreover, as the crack grows the region of stress concentration ahead of the crack tip grows as well, as does the magnitude of the stress peak. The stress peak reaches a certain maximum value (in time) that is uniquely determined by the initial shear stress (ambient shear stress at the beginning of crack propagation) [2]. If the initial shear stress exceeds a certain critical value, the stress peak reaches the shear strength of the material, and a fracture is nucleated slightly ahead of the main crack tip (Abraham and Gao [9] called this a daughter crack). The daughter crack propagates in the intersonic regime [9–12]. The effect of stress-peak-induced acceleration of mode II cracks towards the longitudinal wave speed is quite general and was confirmed numerically and experimentally at various spatial scales from the atomic scale [9,10] to the scale of tectonic faults [11,13]. Despite this basic understanding of the mechanisms of intersonic crack propagation, some fundamental questions concerning the material deformation in the vicinity of the crack tip are still not fully understood. In particular, the physical mechanisms of the formation of a stress concentration region ahead of the crack tip and its stability as well as necessary conditions for the intersonic crack propagation have not yet been completely understood.

In the present paper we will show that the region of concentrated shear stress ahead of the tip dynamically propagating in-plane shear crack is caused by vortexlike elastic displacement of material near the crack tip. This mechanism explains the fact that the region of high shear stress concentration ahead of the crack tip, which propagates faster than the main crack, is specific only to mode II cracks and is not present in other types of cracks [14]. It is well known that circular (vortexlike) patterns of elastic displacement are normally associated with surface waves (Rayleigh, Love, or Lamb waves) and waves propagating along a phase boundary (Stoneley wave) and cannot propagate in the volume of homogeneous materials. However, the formation of a vortexlike structure in homogeneous material is possible if the far-field displacements in the medium have a vortexlike structure. This is not possible in a continuous homogeneous material (with the exception of the trivial case of rigid rotation), but can be realized in a medium with a topological defect such as a dislocation or crack. At the surfaces of a mode II crack, there is a discontinuity of the displacement field, so that the integral of the distortion over a closed loop is nonzero. Uniformly moving vortexlike solutions with this type of topology always tend to form a dislocation-type stress singularity, which is driven by the processes in the elastic far field and do not depend essentially on the details of processes in the immediate vicinity of the singularity. It is intuitively clear that longitudinal waves propagating parallel to the surface of the crack but far away from it will cause circular elastic motion of material points near the crack tip, similarly to vortices in fluids and gases, producing high shear stresses in the crack plane in front of the crack tip. A natural assumption is that this will cause a vortexlike structure with a stress concentration inside it.

To investigate the question of whether the development of the stress peak ahead of the tip of a dynamically growing mode II crack may be caused by vortex-shaped motion of material, we have performed numerical simulations of the wave propagation and cracking process. A specimen containing a

*Corresponding author: sp@ispms.tsc.ru

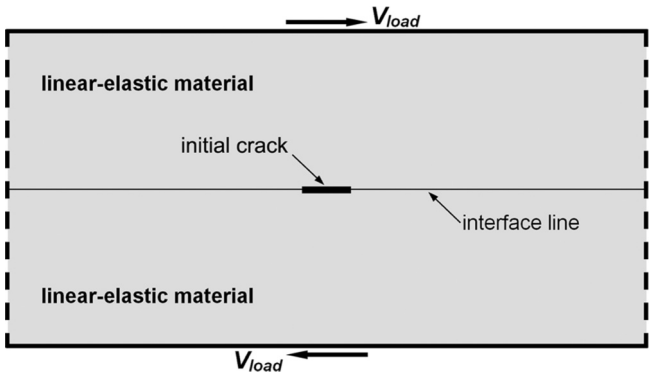

FIG. 1. Schematic representation of the two-dimensional model and the loading conditions. Horizontal solid bold lines delineate the upper and lower external boundaries. Vertical dashed bold lines delineate the vertical faces to which periodic boundary conditions in the horizontal direction are applied. Longitudinal shear loading is introduced by horizontal displacement of the upper and lower external boundaries in opposite directions at a constant velocity V_{load}. The vertical positions of the upper and lower boundaries are fixed.

crack was modeled using the particle-based method of movable cellular automata (MCA). The MCA method is a representative of the group of particle-based numerical discrete element methods (DEM). The DEM were shown to be an effective tool for simulating fractures (including multiple fractures) in the presence of contact interaction of the surfaces [15,16]. The MCA method belongs to the subgroup of simply deformable DEM, in which linear approximation of distribution of displacements in the volume of discrete element is chosen. A specific feature of the MCA, as compared with other representatives of this subgroup of DEM, is its multibody formulation of element interaction forces and potentials [17], which allows for problems of elastic anisotropy, the influence of packaging and the implementation of various models of material response to be dealt with accurately [18]. In the present work the Hubert-Mises criterion (equivalent stress criterion) was used as a local fracture criterion [17]. Plasticity was not taken into account, thus the results are applicable to elastic-brittle materials. An in-depth description of this model and its verification is also to be found in the above-mentioned work [17].

We modeled a two-dimensional slab consisting of two bonded parts (Fig. 1) in the plane-strain-state approximation. Both parts were assumed to be made from the same isotropic, linear-elastic material with Young's modulus $E = 200\,\text{GPa}$, Poisson's ratio $\nu = 0.3$, and density $\rho = 5.7 \times 10^3\,\text{kg/m}^3$. The interface strength (critical equivalent stress $\sigma_{eq}^{is} = 250\,\text{MPa}$) was much smaller than the volume strength of $\sigma_{eq}^{ps} = 2000\,\text{MPa}$. A small initial crack was introduced by means of breaking some bonds between elements at the interface as shown in Fig. 1. Shear loading of the interface was simulated by moving the uppermost and lowermost layers of elements in opposite directions parallel to the interface line with a small constant velocity V_{load}. Periodic boundary conditions were applied in the horizontal direction to avoid the influence of distortions at the boundaries of the slab. In all simulations the horizontal size of the slab was chosen such that elastic waves, which are produced during the dynamic propagation of the

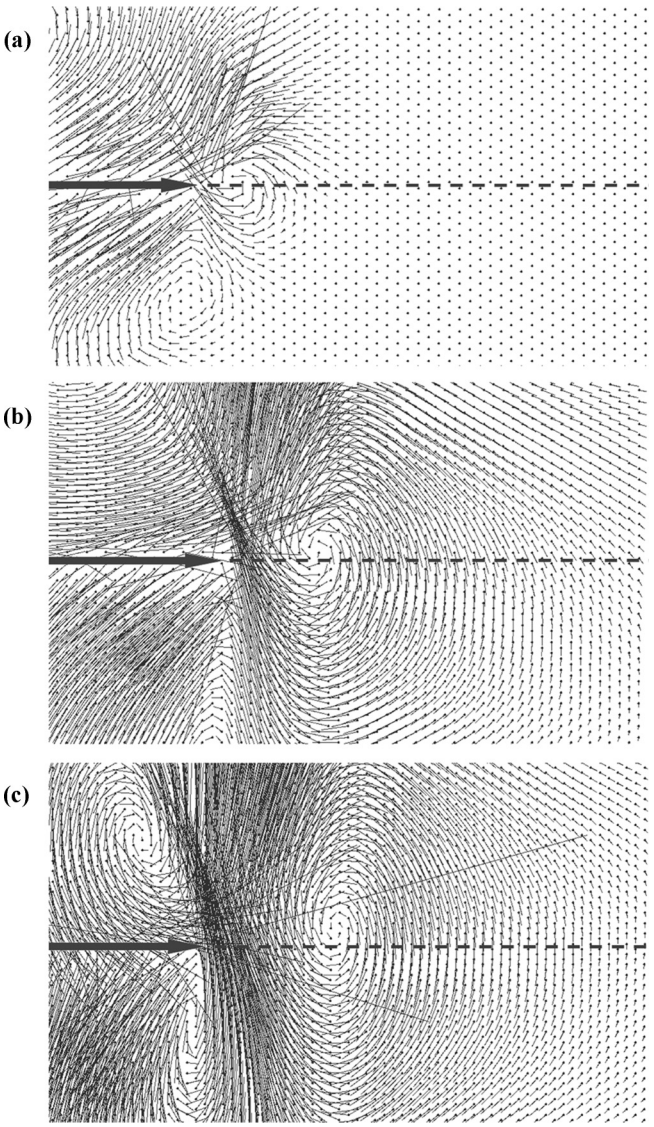

FIG. 2. Velocity field near the tip of the propagating shear crack (a) $0.75\,\mu$s, (b) $3.75\,\mu$s, and (c) $7.5\,\mu$s after the beginning of propagation. Velocity vectors are shown for every third particle in the ensemble. The horizontal arrows mark the position of the plane of the crack and of its right tip. The dashed lines mark intact part of the interface (ahead of the crack tip). In this example the initial crack length was 0.6 mm, the height of the slab was 15 mm, the size of a movable cellular automaton was 0.1 mm, the shear strain rate was $10^{-2}\,\text{c}^{-1}$.

crack tip, do not have time to traverse the entire sample and reach the opposite end of the crack during the simulation.

The deformation of the slab with initial crack proceeds in two stages. In the first stage (before dynamic crack propagation) the system accumulates elastic strain energy. Upon reaching the threshold value of shear stress (shear strength τ_0, which depends on the length of the initial crack) the crack starts to propagate at the interface in the dynamic regime. Figure 2 shows several snapshots of the distribution of particle velocities in the area surrounding the tip of the propagating shear crack. It can be clearly seen that a vortex-shaped motion pattern of material particles (hereafter referred to as elastic

vortex) is formed in the vicinity of the crack from the very beginning of crack propagation.

A detailed analysis of the initial phase of dynamic crack growth has shown that the rotational (vortex) mode of elastic deformation of material ahead of the crack tip arises when a certain critical value of propagation velocity is reached. This critical value is related to the critical velocity introduced in Refs. [19,20] that signifies a change in the character of material deformation in the vicinity of the crack tip. With progressing growth of the crack the elastic vortex involves more and more of the medium ahead of the crack tip [Figs. 2(b)–2(c)].

Note that development of the vortex is inseparably linked to the development of the crack. During the short initial period of crack propagation the crack velocity rapidly increases to a value comparable with the Rayleigh wave speed (this period depends on material and geometrical parameters of the sample and the crack and takes several microseconds in the example shown in Fig. 2) and only changes slightly from then on. These results are in agreement with the findings of other authors [3,4,9,10].

The rotational character of elastic displacements ahead of the crack tip, as seen in our numerical simulations, is also supported by the shape of the asymptotic elastic solution obtained by Mello *et al.* [13]. This solution also exhibits an equal sign of the crack-normal component of velocities on both sides of the crack line and an opposite sign of the crack parallel component. During this initial period the elastic vortex is formed and becomes a self-maintained dynamic object. The propagation velocity of the elastic vortex quickly approaches the shear wave speed V_S. At the same time the crack advances at a velocity lower than the Rayleigh wave speed V_R. Therefore, during the course of propagation the vortex gradually moves away from (and ahead of) the crack tip.

Note that the formation of an elastic vortex at the beginning of dynamic crack propagation is not surprising. Previous studies by the authors have shown that dynamic loading or dynamic change of the stress state of the solid can lead to the formation of elastic vortices near grain or interphase boundaries as well as near free surfaces [21]. In the case of unstable propagation of in-plane shear crack, elastic energy passes to the tip of the crack from fracturing layers of material behind it. Obviously, an influx of mechanical energy sustains the growth of the elastic vortex in the vicinity of the mode II crack.

The spatial confinement of the region of rotational motion ahead of the crack tip and the fact that in this regime the translational velocity of the elastic vortex is equal to the transverse speed of sound V_S led to the conclusion that the region of concentrated shear stress is connected with the elastic vortex. This hypothesis is confirmed by the combined analysis of velocity fields and stress distributions near the tip of a dynamically growing mode II crack. Figure 3(a) shows typical equivalent stress distributions near the tip of a growing crack at different stages of vortex development. A localized region of high shear stresses (compared to the background value far from the crack) accompanies the vortexlike bulk motion of material ahead of the crack tip. This approximately elliptical region is situated in the frontal part of the vortex. The coordinate of the maximum of equivalent stress distribution coincides with the maximum value of the crack-normal component of particle velocities in the frontal part of the vortex. Note that

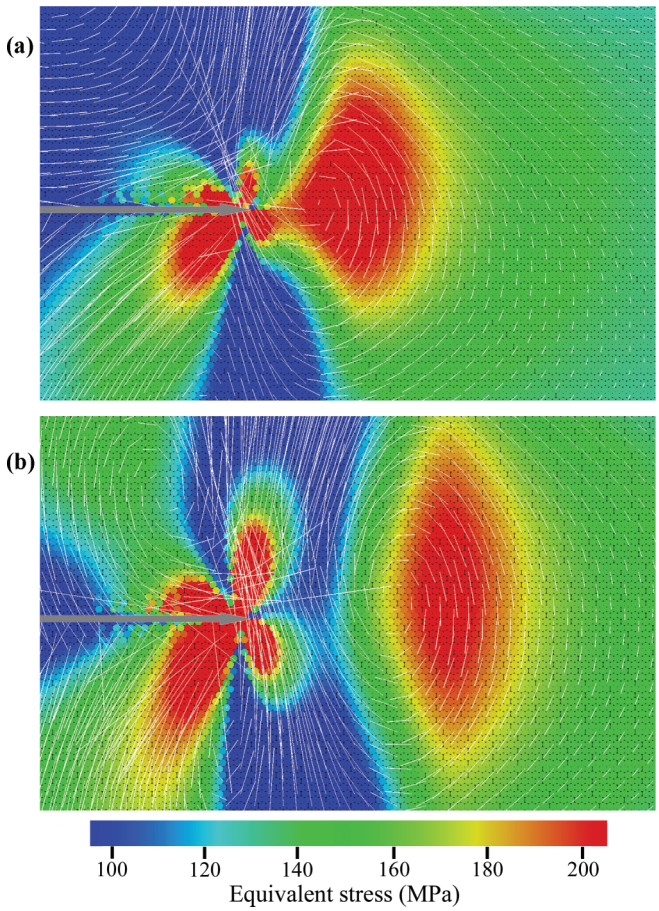

FIG. 3. (Color) Snapshots of the distribution of equivalent stress near the right tip of a growing shear crack (a) 3.75 μs and (b) 7.5 μs after growth start. The system parameters are the same as in Fig. 2. The stress distributions correspond to the time moments shown in Figs. 2(b) and 2(c). The images demonstrate stress patterns before (a) and after (b) detachment of the elastic vortex from the crack. The white lines depict particle velocities.

this coordinate also corresponds to the position of the stress peak ahead of the crack tip as described by Burridge [1] and Andrews [2]. The sustained influx of elastic strain energy enables the expansion of the region ahead of the crack tip that is involved in the elastic vortex motion and in the concentration of shear stress. It was mentioned above, that in the course of propagation the vortex gradually moves away from the crack tip. In the process of evolution of the elastic vortex the concentration of shear stress in it quickly reaches its maximum value and slowly diminishes after that. Combined analysis of the velocity and stress fields have shown that the reduction of the magnitude of the stress peak is related to the detachment of the elastic vortex from the crack and, therefore, loss of an energy source. The snapshots in Fig. 3 show the equivalent stress distributions before [Fig. 3(a)] and after [Fig. 3(b)] the vortex has detached from the crack. The elastic strain energy in the vortex increases until the moment of its separation from the crack (i.e., while the vortex has an energy supply). After separation the elastic vortex becomes a self-contained dynamic object, which propagates independently from its source of origin. During the course of subsequent (independent) vortex

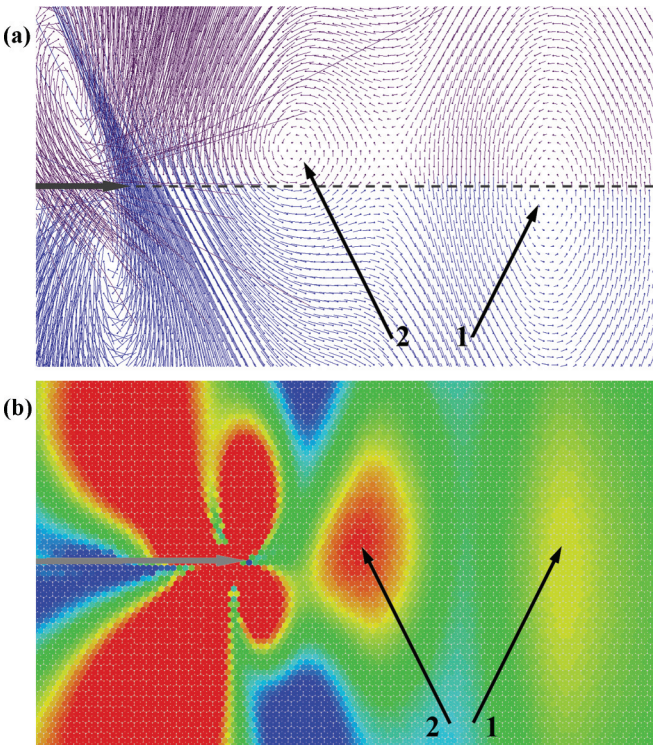

FIG. 4. (Color) (a) Snapshots of the velocity field and (b) the distribution of equivalent stress near the tip of a growing shear crack 15 μs after growth start. The system and initial crack parameters are the same as in Fig. 2. In Fig. 4(a) velocity vectors of automata belonging to the top and bottom halves of the slab are marked by purple and blue colors respectively. In Fig. 4(b) black arrows indicate the first (1) and the second (2) elastic vortices. The images demonstrate velocity and stress patterns just after detachment of the second elastic vortex from the crack.

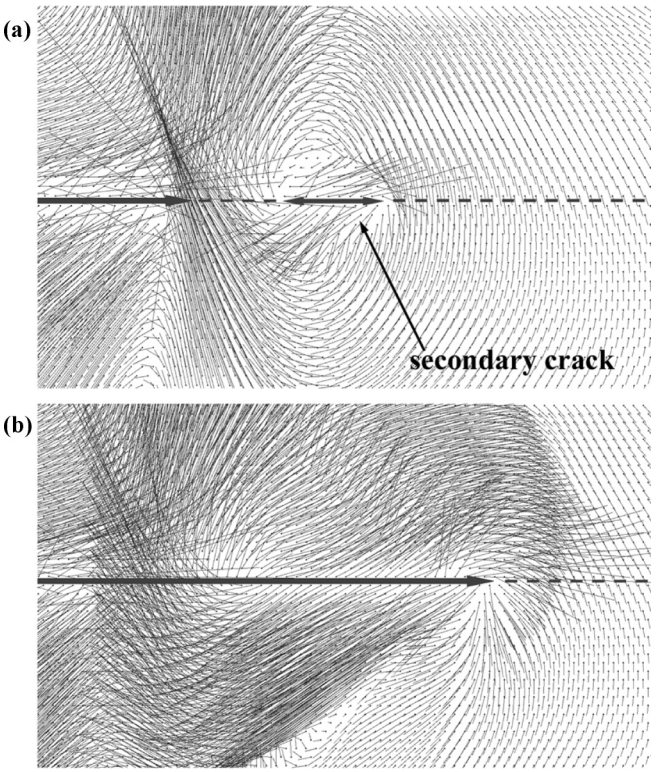

FIG. 5. Velocity field near the tip of the propagating shear crack (a) 0.1 μs and (b) 0.75 μs after the moment of nucleation of the secondary crack at a small distance ahead of the main crack. In this example the initial crack length was 0.5 mm. Other parameters of the model and the value of shear strain rate are the same as in the example shown in Figs. 2–4.

propagation the concentration of shear stresses gradually decreases since the influx of elastic energy is interrupted.

Because of continuous influx of elastic strain energy to the tip of a dynamically propagating crack from fracturing layers of material behind it, a new vortex starts to form at the crack tip after the previous one detaches. The development of the new vortex and its direction of rotation are analogous to the previous vortex. The second vortex also propagates at shear wave velocity (faster than the crack) and gradually moves away from the crack tip. The maximum concentration of equivalent stress in the second vortex is achieved at the moment of its separation from the crack (this moment is shown in Fig. 4). After that the second vortex travels independently on the crack (it follows the first one) and gradually attenuates since the influx of elastic energy is interrupted. Then the third elastic vortex begins to develop and so on. Hence, a mode II crack propagating in conventional sub-Raleigh regime generates a chain of elastic vortices moving ahead of the crack tip at the shear wave speed V_s. An important feature of these vortices is the shear stress concentration in their frontal parts. It should be noted that, although consecutive vortices are similar in shape and evolution, there are quantitative differences in some parameters. One of these parameters is the concentration of equivalent stresses in the elastic vortex, in particular, the maximum equivalent stress $\sigma_{eq}^{\max}$ that is reached in the center of the elliptical region of high shear stress at the moment of vortex detachment from the crack. Analysis of simulation results shows that the highest value of $\sigma_{eq}^{\max}$ is reached in the first elastic vortex (that is formed at the beginning of dynamic crack growth), while subsequent vortices have slightly lower values of $\sigma_{eq}^{\max}$ (up to 10%) than its predecessor. The reduction of stress concentration in subsequent vortices can be seen by comparing Figs. 3 and 4.

The magnitude of shear stress concentration in the elastic vortex determines the possibility of acceleration of a mode II crack to intersonic regime. Such acceleration becomes possible if the magnitude of shear stresses in the frontal part of the first, strongest elastic vortex reaches the shear strength of the interface before the moment of detachment ($\sigma_{eq}^{\max} > \sigma_{eq}^{is}$). In this case a short secondary crack nucleates at a small distance ahead of the main crack, at the center of the region of high shear stresses [Fig. 5(a)]. This secondary crack then merges with the main crack and the entire rupture propagates at a velocity comparable with the longitudinal wave speed [Fig. 5(b)]. Note that nucleation of the secondary crack leads to destruction of the elastic vortex that produced it. As can be seen in Fig. 5(b), the crack propagating in the intersonic regime radiates a strong longitudinal wave [4,6,9,13] and cannot nucleate new elastic vortices, because it propagates faster than the shear wave speed. Hence, depending on the magnitude of $\sigma_{eq}^{\max}$ (which

is a function of initial conditions), the mode II crack stably propagates in the conventional sub-Raleigh regime, generating a series of elastic vortices (at $\sigma_{eq}^{\max} < \sigma_{eq}^{is}$), or accelerates towards the longitudinal wave speed shortly after the start of dynamic propagation (before separation from the first elastic vortex, at $\sigma_{eq}^{\max} > \sigma_{eq}^{is}$).

Note that within the considered elastic-brittle material model the possibility of irreversible deformation and localized dissipation of elastic strain energy is not considered. In such a model the main condition for crack acceleration to intersonic regime is that the initial shear stress τ_0 (ambient shear stress at the beginning of crack propagation) exceeds a certain critical value. In other words, the shear strength of the material in the frontal part of the elastic vortex must be reached. The magnitude of the critical value is determined by the elastic material parameters and the strength of the interface. At the same time, in real materials, intense localized dissipation of energy may take place in the vicinity of the crack tip. In models of brittle materials this can be taken into account, e.g., through the decohesion-weakening effect [2,4]. Obviously, in this case, the critical value of initial shear stress will be a function of the parameters of decohesion-weakening model and friction law. Note also that in materials in which ductility is determined by the evolution of an ensemble of defects in the crystal lattice, the elastic vortices can initiate rotational inelastic displacements ahead of the crack tip.

Finally, we would like to discuss the initial conditions under which the acceleration of a crack in a brittle solid to an intersonic speed takes place. Analytical models of dynamic growth of mode II cracks regard the steady-state regime of this process as self-similar [1,22]. This means that the elastic vortices propagating ahead of the crack tip must be scale invariant. This suggestion was confirmed by special numerical experiments, with different slabs obtained by scaling the sample in Fig. 1 within several orders of magnitude. The scaling was performed by changing the size of the movable cellular automata and proportional scaling of the sample and the initial crack while preserving its ratios. Simulation results have shown that the extensive parameters of elastic vortices (including the time from the nucleation of the vortex to detachment from the crack, the geometrical characteristics of the vortex at different stages of its development, as well as the stress and strain gradients) scale in proportion to spatial scaling, while intensive parameters (stresses and velocities in corresponding areas) remain the same in all cases. This confirms the scale-invariant character of elastic vortices ahead of the tip of mode II cracks propagating in the sub-Rayleigh regime.

Moreover, the scale-invariant character of the elastic vortex shows that the criterion determining the possibility of acceleration of a mode II crack to supershear velocity must be an intensive parameter of the system state. The traditionally used criterion is the initial shear stress, in other words the shear strength τ_0 of the material with a preexisting structural defect (which is a fraction of the shear strength of intact material) [2]. This relation is fairly obvious because the liberation and redistribution of elastic strain energy during dynamic crack propagation is driven by previously accumulated energy, which only depends on τ_0 (our results have shown a linear dependency between $\sigma_{eq}^{\max}$ and τ_0). Given the utilized loading scheme, τ_0 is uniquely determined by the geometric characteristics of the initial defect (in the considered problem—the length L_0 and thickness D of the initial crack). Therefore the geometrical characteristics of the initial crack can be used as criteria for the propagation of a crack in intersonic regime along with τ_0. Additionally, due to the scale invariance of the elastic vortex, the geometrical criterion must take the form of a dimensionless combination of the dimensional geometrical crack parameters.

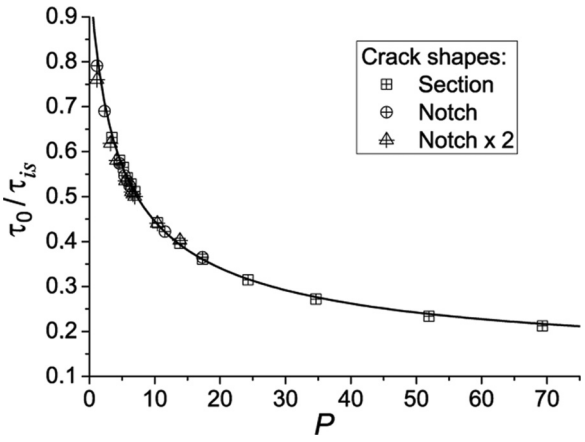

FIG. 6. Dependence of shear strength of the interface with initial crack τ_0 on dimensionless geometrical crack parameter P. Shear strength τ_0 is normalized to the value of strength of the intact interface τ_{is}. Points show numerically determined values of shear strength for the interface with different kinds of cracks (section and two notches with doubly different thicknesses). Solid line shows empirically determined approximation (1).

The simplest analytical model linking τ_0 with the geometrical characteristics of the initial crack is the Griffith crack theory [23]. Within the Griffith model this dependence takes the following form: $\tau_0 \propto \tau_{is}\sqrt{r_0/L_0}$, where r_0 is the interatomic distance (it was supposed that the roughness of the crack is determined by the packing of atoms and is proportional to r_0). This equation does determine the dimensionless geometrical parameter of the initial crack (L_0/r_0), but is only applicable for cracks of atomic thickness in a region $L_0 > r_0$. We have obtained a more general relation of this kind for mode II cracks of arbitrary effective thickness D. We considered two types of initial cracks at the interface: section (realized by removing connections between adjacent automata from different slabs of the specimen) and notch (realized by removing layers of elements on both sides of the interface line). In both cases the parameter D is determined as the distance between the centers of the elements of the opposing surfaces. The length of the initial crack L_0 was varied in a wide range from 0 (intact interface) to $L_0 = 100D$. Our numerical experiments have shown that the shear strength of the interface with initial crack τ_0 depends only on the dimensionless geometrical parameter $P = L_0/D$ (Fig. 6).

The numerically determined dependence $\tau_0(P)$ is approximated well by the empirical equation

$$\tau_0 = \tau_{is}\sqrt{\frac{1}{1+\alpha P}\left[1-\left(\frac{\tau_\infty}{\tau_{is}}\right)^2\right]+\left(\frac{\tau_\infty}{\tau_{is}}\right)^2} \qquad (1)$$

where $\tau_{is} = \sigma_{eq}^{is}/\sqrt{3}$ is the shear strength of the intact interface, $\tau_\infty \approx 0.1\tau_{is}$ is the shear strength of semi-infinite crack, α is a constant depending on material properties ($\alpha \approx 0.45$ for

the considered material parameters). The empirically derived expression (1) can be considered as a generalization of the conventional Griffith expression for cracks with arbitrary lengths and effective thicknesses. The value of τ_0 is equal to the shear strength of intact material τ_{is} at $P = 0$ (no initial crack) and converges to the shear strength of a semi-infinite crack τ_∞ at $P \to \infty$ (i.e., at $L_0 \to \infty$, because the effective thickness D cannot be infinitely small), while in the characteristic interval $1 < P < (\tau_{is}/\tau_\infty)$ the character of change of τ_0 is very close to Griffith's analytical prediction (remember that $L_0 > D$ is the range of definition of Griffith's expression).

The dependence (1) has fundamental significance for understanding of the geometrical conditions necessary for in-plane shear (mode II) crack acceleration towards the speed of longitudinal wave. As was shown directly or indirectly by other authors, this acceleration takes place when the initial crack length is less than some threshold value [2,5,9]. The simulation results presented above show that the possibility of reaching the critical magnitude of the stress peak is determined by the quantity of normalized length parameter P. If the initial crack is characterized by the magnitude of the dimensionless parameter $P > P_{\text{crit}}$ (where P_{crit} is the value, at which the peak stress at the interface ahead of the crack reaches the interface strength), the crack can only propagate in the conventional sub-Rayleigh regime. If $P < P_{\text{crit}}$, then the crack can, in principle, overcome the Rayleigh wave velocity barrier. This means that only cracks whose initial length is $L_0 < L_{\text{crit}} = DP_{\text{crit}}$ are capable of propagating in the intersonic regime. Our simulation results have shown the quantity P_{crit} is material dependent. For elastic-brittle materials it varies from 1–10. For elastic-plastic materials P_{crit} is significantly smaller.

The present paper complements numerous numerical and laboratory studies of dynamic mode II fracture. It shows that an elastic vortex developing ahead of a dynamically propagating mode II crack serves as a physical mechanism of formation of a confined region of high shear stresses at some distance from the crack tip and hence is responsible for shear crack acceleration towards longitudinal wave speed. The elastic vortex is a scale-invariant dynamic object, which explains the generality of the dependencies governing the propagation of longitudinal shear cracks at different scales and, in particular, the well-known fact that the supershear regime of shear crack propagation is observed at all scales. The relationship between the dimensionless geometrical parameter of the initial crack P and the maximum magnitude of the stress peak ahead of the mode II crack tip makes it possible to predict the potential of existing cracks in brittle materials to propagate in the supershear regime.

E.V.S. and V.L.P. gratefully acknowledge financial support from the Russian Science Foundation Grant No. 14-19-00718 (Russia). M.V.P. acknowledges financial support from The Tomsk State University Academician D. I. Mendeleev Fund Program (research Grant No. 8.2.19.2015).

[1] R. Burridge, Admissible speeds for plane-strain self-similar shear cracks with friction but lacking cohesion, J. R. Astr. Soc. **35**, 439 (1973).
[2] D. J. Andrews, Rupture velocity for plane strain shear cracks, J. Geophys. Res. **81**, 5679 (1976).
[3] Z. Shi, Y. Ben-Zion, and A. Needleman, Properties of dynamic rupture and energy partition in a solid with a frictional interface, J. Mech. Phys. Solids **56**, 5 (2008).
[4] S. Hao, W. K. Liu, P. A. Klein, and A. J. Rosakis, Modeling and simulation of intersonic crack growth, Int. J. Solids Struct. **41**, 1773 (2004).
[5] P. H. Geubelle and D. V. Kubair, Intersonic crack propagation in homogeneous media under shear-dominated loading: Numerical analysis, J. Mech. Phys. Solids **49**, 571 (2001).
[6] A. J. Rosakis, Intersonic shear cracks and fault ruptures, Adv. Phys. **51**, 1189 (2002).
[7] E. M. Dunham, Conditions governing the occurrence of supershear ruptures under slip-weakening friction, J. Geophys. Res. **112**, B07302 (2007).
[8] O. Ben-David, G. Cohen, and J. Fineberg, The dynamics of the onset of frictional slip, Science **330**, 211 (2010).
[9] F. F. Abraham and H. Gao, How fast can cracks propagate?, Phys. Rev. Lett. **84**, 3113 (2000).
[10] F. F. Abraham, The atomic dynamics of fracture, J. Mech. Phys. Solids **49**, 2095 (2001).
[11] K. Xia, A. J. Rosakis, and H. Kanamori, Laboratory earthquakes: The sub-Rayleigh-to-supershear rupture transition, Science **303**, 1859 (2004).
[12] F. Barras, D. S. Kammer, P. H. Geubelle, and J.-F. Molinary, A study of frictional contact in dynamic fracture along bimaterial interface, Int. J. Fract. **189**, 149 (2014).
[13] M. Mello, H. S. Bhat, A. J. Rosakis, and H. Kanamori, Identifying the unique ground motion signatures of supershear earthquakes: Theory and experiments, Tectonophysics **493**, 297 (2010).
[14] K. B. Broberg, Differences between mode I and mode II crack propagation, Pure Appl. Geophys. **163**, 1867 (2006).
[15] G. G. W. Mustoe, A generalized formulation of the discrete element method, Engineering Computations **9**, 181 (1992).
[16] L. Jing and O. Stephansson, *Fundamentals of Discrete Element Methods for Rock Engineering* (Elsevier, Amsterdam, 2007).
[17] S. G. Psakhie, E. V. Shilko, A. S. Grigoriev, S. V. Astafurov, A. V. Dimaki, and A. Yu. Smolin, Smolin, A mathematical model of particle-particle interaction for discrete element based modeling of deformation and fracture of heterogeneous elastic-plastic materials, Eng. Fract. Mech. **130**, 96 (2014).
[18] V. L. Popov and S. G. Psakhie, Theoretical principles of modeling elastoplastic media by movable cellular automata method. I. Homogeneous media, Phys. Mesomechanics **4**(1), 15 (2001).
[19] M. Adda-Bedia, R. Arias, M. Ben Amar, and F. Lund, Dynamic instability of brittle fracture, Phys. Rev. Lett. **82**, 2314 (1999).
[20] M. Adda-Bedia, R. Arias, M. Ben Amar, and F. Lund, Generalized Griffith criterion for dynamic fracture and the stability of crack motion at high velocities, Phys. Rev. E **60**, 2366 (1999).
[21] S. G. Psakhie, K. P. Zolnikov, A. I. Dmitriev, A. Yu. Smolin and E. V. Shilko, Dynamic vortex defects in deformed material, Phys. Mesomech. **17**, 15 (2014).
[22] K. B. Broberg, The propagation of a brittle crack, Arkiv for Fysik (Stockholm) **18**, 159 (1960).
[23] A. A. Griffith, The phenomena of rupture and flow in solids, Philos. Trans. R. Soc. London A **221**, 163 (1921).